SUPPLEMENTAL FIGURE 1

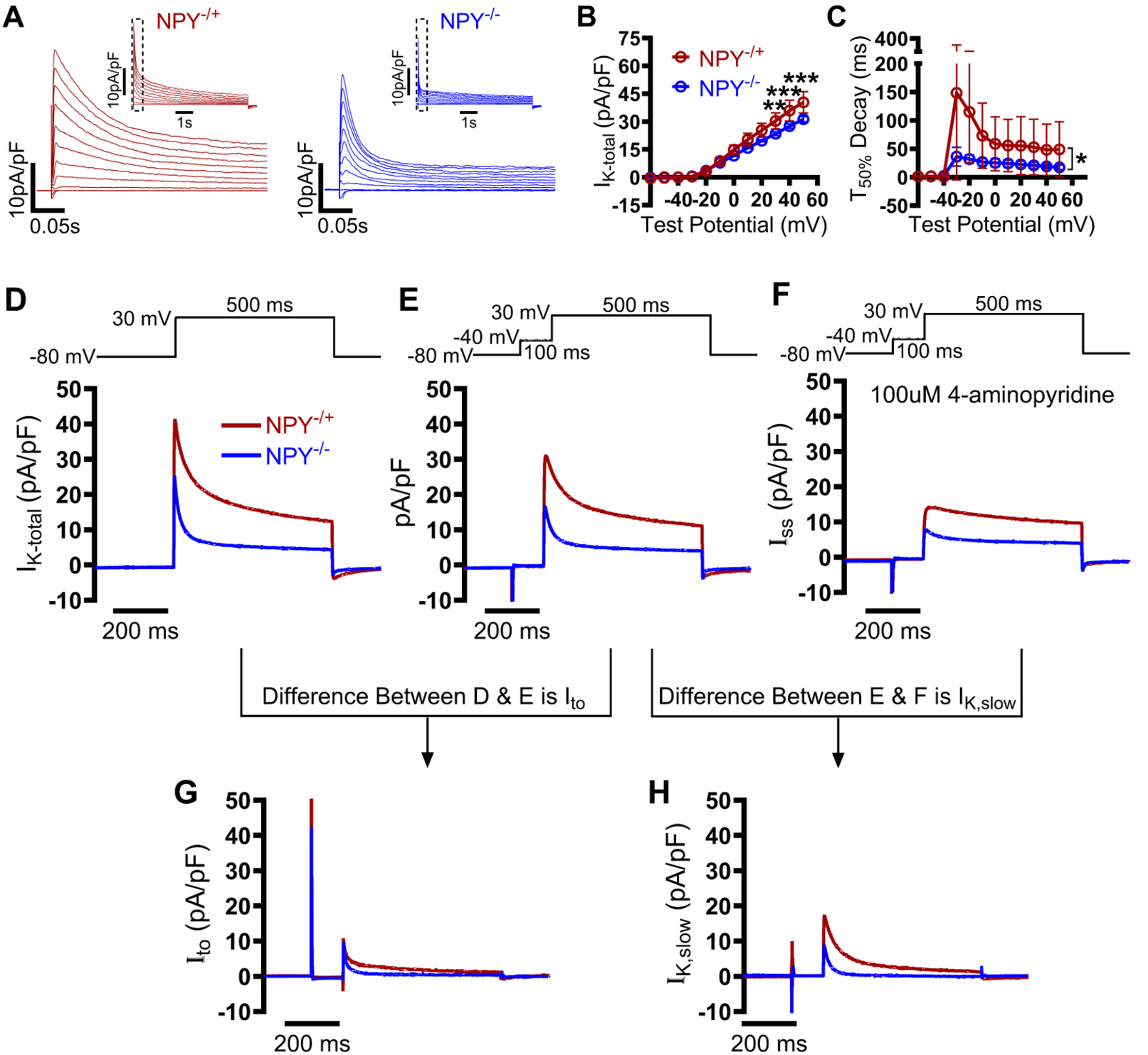

Supplemental Figure 1. NPY depletion alters outward K^+ current properties in ventricular cardiomyocytes. (A) Representative traces of total outward potassium current ($I_{K\text{-}total}$) recorded at varying test potentials in $NPY^{-/+}$ and $NPY^{-/-}$ ventricular cardiomyocytes. **(B)** Current-voltage relationship plot of $I_{K\text{-}total}$. **(C)** Time to ½ inactivation of $I_{K\text{-}total}$. **(D)** Representative traces of $I_{K\text{-}total}$ recorded in both groups using the voltage-clamp protocol shown above the traces. Cells were depolarized from a holding potential of −80 mV to +30 mV for 500 ms. **(E)** Representative current traces recorded using an inactivating prepulse protocol (−40 mV for 100 ms) to inactivate transient outward potassium current (I_{to}) before the test pulse to +30 mV. Under these conditions, the remaining current represents $I_{K\text{-}total}$ without I_{to}. **(F)** Representative traces recorded in the presence of 100 µM 4-aminopyridine (4-AP) to inhibit slowly inactivating potassium current ($I_{K,slow}$). The residual current under these conditions represents the steady-state potassium current (I_{ss}). **(G)** I_{to} obtained by digital subtraction of currents in panel E from those in D (D − E). I_{to} density was comparable between $NPY^{-/+}$ and $NPY^{-/-}$ cardiomyocytes. **(H)** $I_{K,slow}$ obtained by subtracting currents in panel **F** from those in **E** (E − F). $I_{K,slow}$ was reduced in $NPY^{-/-}$ cardiomyocytes compared with $NPY^{-/+}$ control. Currents are normalized to cell capacitance and expressed as current density (pA/pF). Data are mean ± SD, with cardiomyocytes nested within mice and mice treated as the experimental unit; *$p < 0.05$, **$p < 0.01$, ****$p < 0.0001$.

SUPPLEMENTAL FIGURE 2

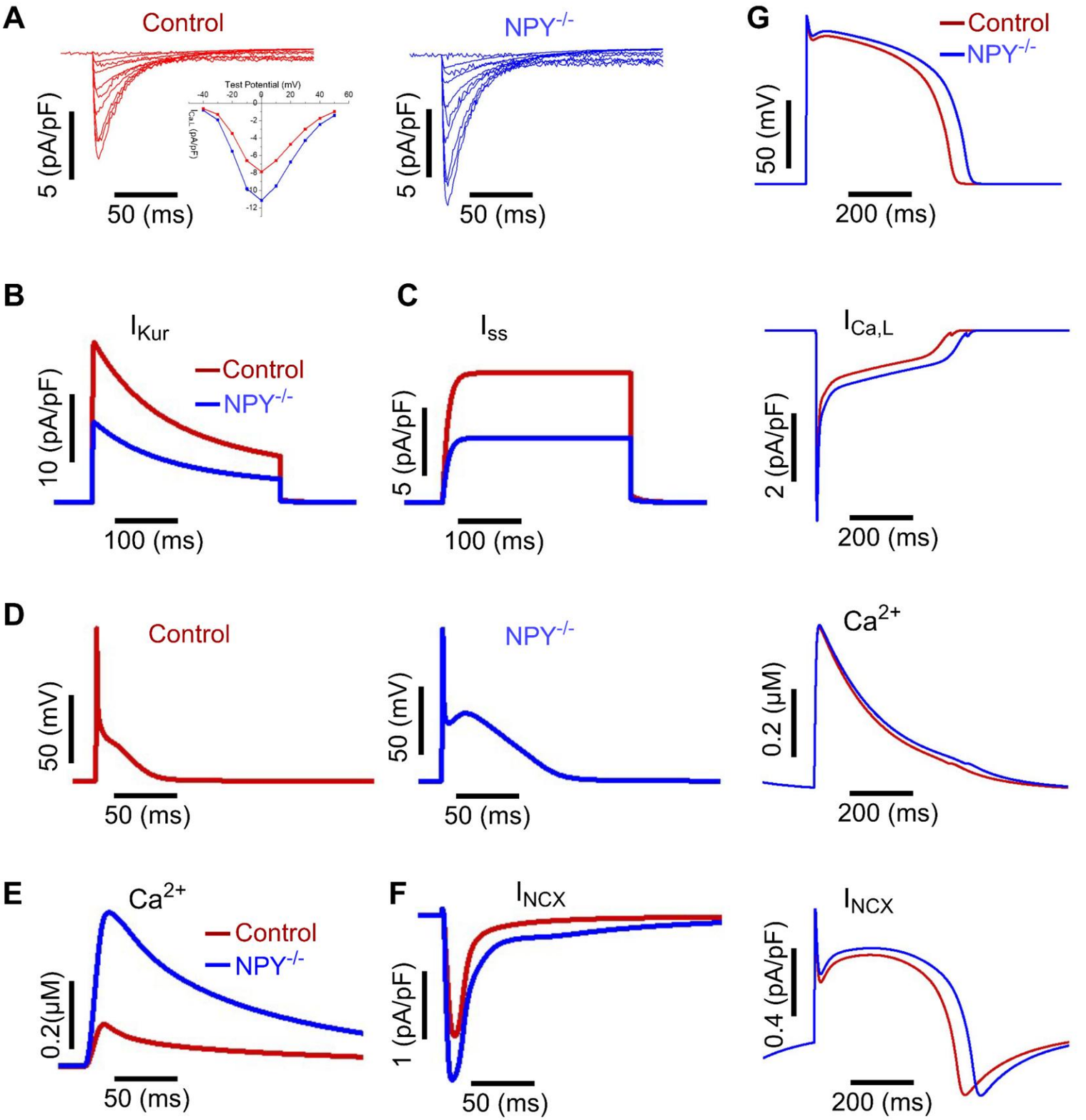

Supplemental Figure 2. Computational modeling of altered $I_{Ca,L}$, $I_{K,slow}$, and I_{ss} reproduces AP changes in NPY$^{-/-}$ cardiomyocytes and predicts corresponding effects in human ventricular myocytes. (A) simulated $I_{Ca,L}$ in control and NPY$^{-/-}$ cardiomyocytes showing increased current density in NPY$^{-/-}$. **(B and C)** simulated $I_{K,slow}$ and I_{ss} in control and NPY$^{-/-}$ cardiomyocytes showing reduced current density in NPY$^{-/-}$. **(D)** simulated control and NPY$^{-/-}$ mice ventricular myocyte AP generated by 33% increase in $I_{Ca,L}$, 50% reduction in $I_{K,slow}$ and I_{ss} reproduce the APD prolongation observed experimentally. **(E)** intracellular Ca transient ([Ca]i) recorded from the simulated mice AP showing increased amplitude in NPY$^{-/-}$ myocytes. (F, sodium/calcium exchanger current (I_{NCX}) recorded from the simulated mice AP showing enhanced current in NPY$^{-/-}$ consistent with increased [Ca]i. **(G)** simulated effects of NPY depletion in human ventricular AP models generated by 40% increase in $I_{Ca,L}$ showing prolonged APD in endocardial cells with corresponding $I_{Ca,L}$, [Ca]i and I_{NCX}.

SUPPLEMENTAL FIGURE 3

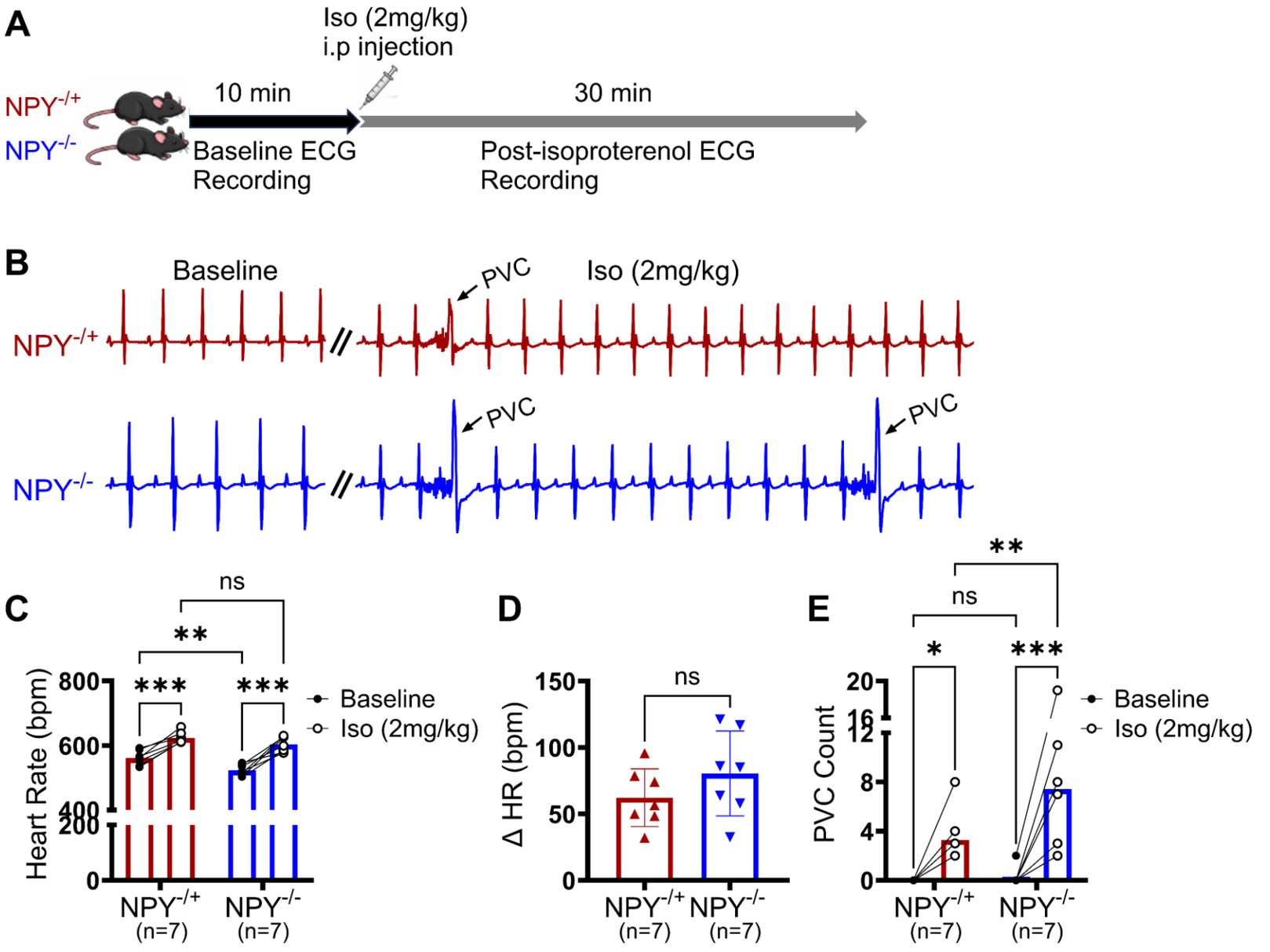

Supplemental Figure 3. NPY deficiency increases susceptibility to isoproterenol-induced ventricular ectopy. (A) Experimental protocol for in vivo electrocardiogram (ECG) recordings. Baseline ECGs were recorded for 10 min in mice followed by intraperitoneal injection of isoproterenol (Iso, 2 mg/kg) and ECG monitoring for an additional 30 min. **(B)** Representative ECG traces from $NPY^{-/+}$ and $NPY^{-/-}$ mice at baseline and after Iso administration. Premature ventricular complexes (PVCs) are indicated. **(C)** Quantification of heart rate at baseline and following Iso injection in $NPY^{-/+}$ and $NPY^{-/-}$ mice. **(D)** Change in heart rate (ΔHR) following Iso administration in $NPY^{-/+}$ and $NPY^{-/-}$ mice. **(E)** Quantification of PVC events observed during the recording period at baseline and after Iso injection. Iso induced significantly more PVCs in $NPY^{-/-}$ mice compared with $NPY^{-/+}$ mice. Data are mean ± SD; *p < 0.05, **p < 0.01, ***p < 0.001.

SUPPLEMENTAL FIGURE 4

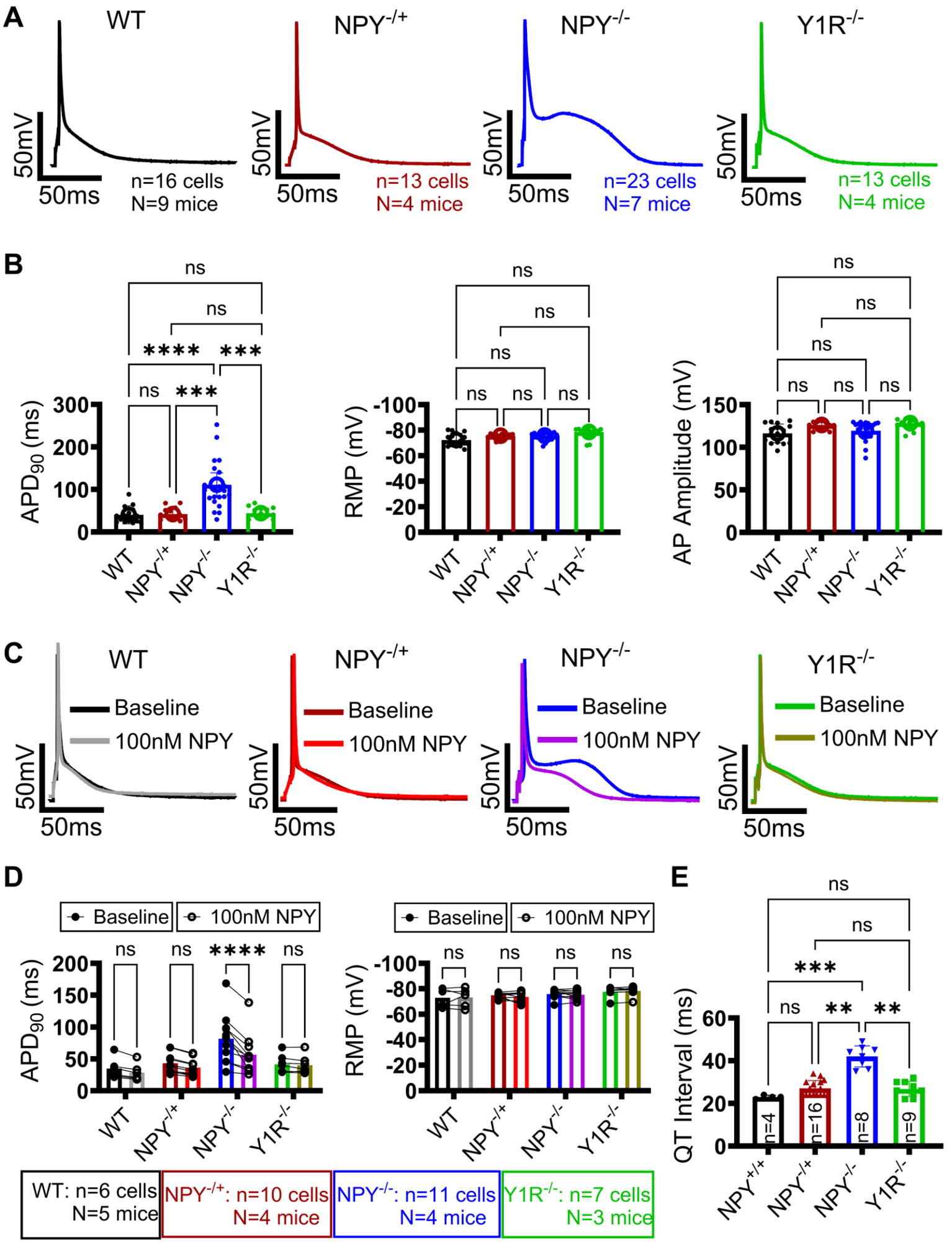

Supplemental Figure 4. NPY depletion-induced ventricular repolarization abnormalities are independent of Y1 receptor (Y1R) signaling. (A) Representative ventricular cardiomyocyte action potentials recorded from WT, $NPY^{-/+}$, $NPY^{-/-}$, and $Y1R^{-/-}$ mice under baseline conditions. **(B)** Quantification of AP duration at 90% repolarization (APD_{90}), resting membrane potential (RMP), and AP amplitude. APD_{90} was prolonged in $NPY^{-/-}$ cardiomyocytes, whereas $Y1R^{-/-}$ cells exhibited values comparable to controls. **(C)** Representative action potentials before and after application of 100 nM NPY. **(D)** Paired analysis of APD_{90} and RMP before and after 100 nM NPY treatment. Exogeneous NPY significantly shortened APD in $NPY^{-/-}$ cardiomyocytes but not in $Y1R^{-/-}$ cells. **(E)** QT interval measurements from surface ECG recordings. Unlike $NPY^{-/-}$ mice, $Y1R^{-/-}$ mice showed QT intervals comparable to controls, indicating that ventricular electrophysiological abnormalities induced by NPY depletion are not mediated through Y1R signaling. Data are mean ± SD, with cardiomyocytes nested within mice and mice treated as the experimental unit; $^{**}p < 0.01$, $^{***}p < 0.001$, $^{****}p < 0.0001$.